ADVANCES IN ATMOSPHERIC SCIENCES, VOL. 37, JULY 2020, 1–8

• **News & Views** •

Could the Recent Taal Volcano Eruption Trigger an El Niño and Lead to Eurasian Warming?

Fei LIU*[1,2,3], Chen XING[3], Jinbao LI[4], Bin WANG[5], Jing CHAI[3], Chaochao GAO[6], Gang HUANG[7], Jian LIU[8], and Deliang CHEN[9]

[1]*School of Atmospheric Sciences and Guangdong Province Key Laboratory for Climate Change and Natural Disaster Studies*, *Sun Yat-sen University*, *Zhuhai* 519082, *China*

[2]*Southern Marine Science and Engineering Guangdong Laboratory (Zhuhai)*, *Zhuhai* 519082, *China*

[3]*Earth System Modeling and Climate Dynamics Research Center*, *Nanjing University of Information Science and Technology*, *Nanjing* 210044, *China*

[4]*Department of Geography*, *University of Hong Kong*, *Pokfulam*, *Hong Kong*

[5]*Department of Atmospheric Sciences and International Pacific Research Center*, *University of Hawaii at Manoa*, *Honolulu*, *HI* 96822, *USA*

[6]*Department of Environmental Science*, *Zhejiang University*, *Hangzhou* 310058, *China*

[7]*State key Laboratory of Numerical Modeling for Atmospheric Sciences and Geophysical Fluid Dynamics*, *Institute of Atmospheric Physics*, *Chinese Academy of Sciences*, *Beijing* 100029, *China*

[8]*Key Laboratory for Virtual Geographic Environment*, *Ministry of Education*; *Jiangsu Provincial State Key Laboratory Cultivation Base of Geographical Environment Evolution*; *School of Geography Science*, *Nanjing Normal University*, *Nanjing* 210023, *China*

[9]*Department of Earth Sciences*, *University of Gothenburg*, *Gothenburg* 405 30, *Sweden*

(Received 19 February 2020; revised 28 March 2020; accepted 1 April 2020)

Citation: Liu, F., and Coauthors, 2020: Could the recent Taal Volcano eruption trigger an El Niño and lead to Eurasian warming? *Adv. Atmos. Sci.*, **37**(7), https://doi.org/10.1007/s00376-020-2041-z. (in press)

The Taal Volcano in Luzon is one of the most active and dangerous volcanoes of the Philippines. A recent eruption occurred on 12 January 2020 (Fig. 1a), and this volcano is still active with the occurrence of volcanic earthquakes. The eruption has become a deep concern worldwide, not only for its damage on local society, but also for potential hazardous consequences on the Earth's climate and environment.

Volcanic eruptions affect climate through injecting sulfur dioxide (SO_2) into the stratosphere (Robock, 2000). The volcanic sulfate aerosols formed through the reaction between SO_2 and hydroxide or water vapor exhibit a typical *e*-folding time of about 12−14 months. A large eruption that injects sulfate aerosols into the stratosphere can perturb global climate by scattering incoming solar radiation, resulting in global surface cooling that may last for two to three years after the eruption owing to the delayed ocean response (Sear et al., 1987; Robock, 2000). Tropical eruptions tend to slow down the global hydrological cycle (Trenberth and Dai, 2007; Iles and Hegerl, 2014), leading to a weakened global monsoon system (Man and Zhou, 2014; Liu et al., 2016; Stevenson et al., 2016). The semi-arid region, however, tends to get wetter owing to the monsoon−desert coupling mechanism (Zuo et al., 2019).

Big volcano eruptions' climate impacts can last for decades through a positive sea-ice/albedo feedback, even though the volcanic aerosols in the stratosphere remain only for about a year (Schneider et al., 2009; Zanchettin et al., 2011; Slawinska and Robock, 2018). Expanded Arctic sea-ice cover existed for a decade after the latest three large tropical eruptions, although the sea ice is sensitive to pre-eruption temperature (Gagné et al., 2017). One of the largest eruptions during the current Holocene Epoch, the 1258 Samalas eruption, together with three small ensuing eruptions, are speculated to have triggered the Little Ice Age through positive sea-ice/ocean feedbacks during a cooling summer (Miller et al., 2012). The

* Corresponding author: Fei LIU
Email: liuf@nuist.edu.cn

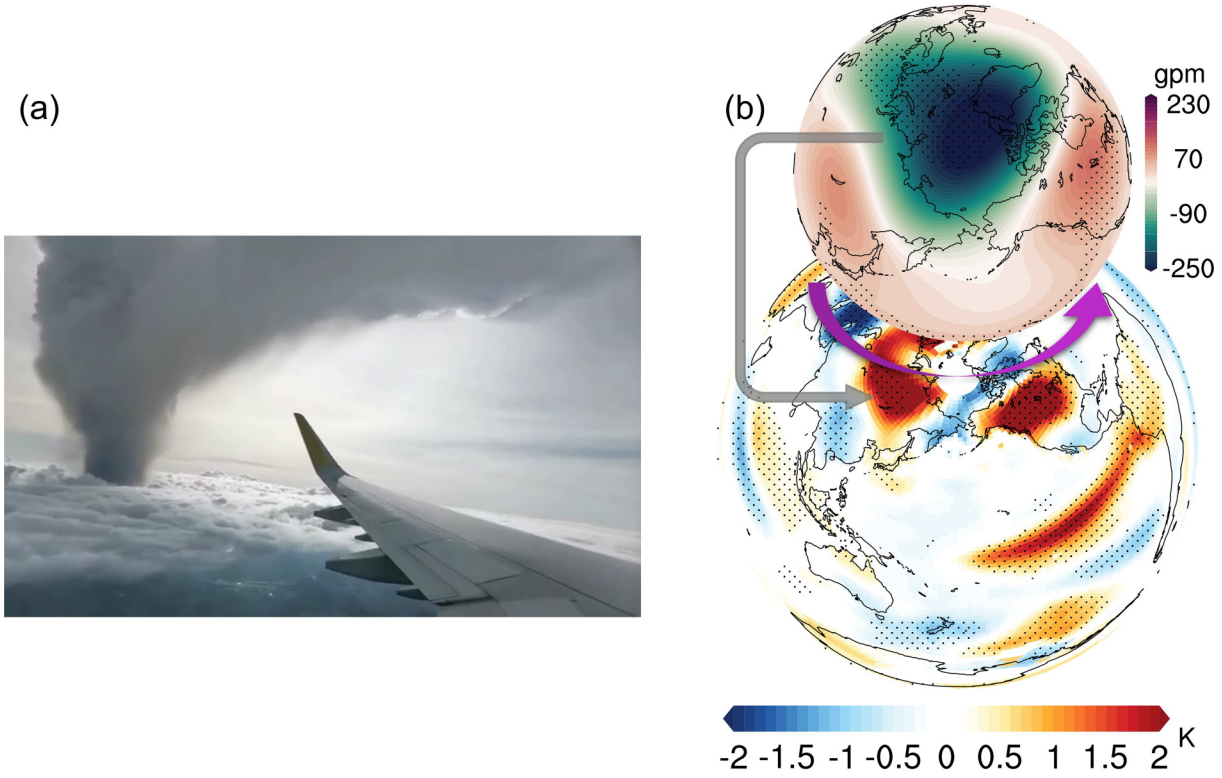

Fig. 1. Observed El Niño and enhanced polar vortex–induced Eurasian warming after three large tropical eruptions. (a) Eruption cloud of the Taal Volcano taken from an airplane on 12 January 2020 (Photo credit: Faxin CHEN). (b) Composite 50-hPa geopotential height anomaly in JRA-55 (upper panel) and surface air temperature anomaly in GISTEMP in the first boreal winter following the 1963 Agung, 1982 El Chichón, and 1991 Pinatubo eruptions [updated from Xing et al. (2020)]. Stippling indicates temperature anomalies significant at the 95% confidence level. The magenta arrow denotes stratospheric westerly anomalies around 70°N, and the gray arrow gives the potential linkage between the stratosphere and surface.

phase of the Atlantic Multidecadal Oscillation can be affected by large volcanic eruptions (Otterå et al., 2010). Background conditions, i.e., the initial climate state and additional external forcings, may influence the decadal responses of oceanic heat transport and sea ice in the North Atlantic to large tropical eruptions (Zanchettin et al., 2011, 2013). However, in work by Bethke et al. (2017), historical volcanic eruptions could not counteract the long-term global warming trend induced by anthropogenic greenhouse gases under the future emissions scenario based on a general circulation model (GCM) simulation.

Nevertheless, volcanic eruption-induced global cooling suggests a useful strategy against global warming (Niemeier and Tilmes, 2017). Stratospheric aerosol geoengineering (SAG), also known as "solar radiation management" in the Geoengineering Model Intercomparison Project (GeoMIP), is an analogue of large volcanic eruptions in terms of impacts on global climate, and an artificial supplementary method that could mitigate anthropogenic global warming through increasing the planetary albedo (Kravitz et al., 2015; Niemeier and Tilmes, 2017). The goal to hold temperatures at 1.5°C or 2.0°C higher than the level of 1850–1900 can be reached with SAG, which partially balances a future high emissions scenario with CESM2 (WACCM6) (Tilmes et al., 2019). Apart from the high economic costs and technological requirements for SAG, one more obstacle is that its direct and indirect effects on the hydrological cycle remain inconsistent. For the same global temperature change, volcanic eruption-induced global precipitation changes are stronger than those resulted from greenhouse gases (Liu et al., 2018c). Although precipitation and evaporation are reduced by applying SAG (Tilmes et al., 2013), it is inspiring that wetlands, as the ratio of precipitation and evaporation, can be increased over major American land regions where people reside (Xu et al., 2020).

Five large tropical eruptions have occurred since instrumental observations began to become available 150 years ago (Sato et al., 1993; Gao et al., 2008), i.e., the 1883 Krakatau, 1902 Santa Maria, 1963 Agung, 1982 El Chichón, and 1991 Pinatubo eruptions (Table 1). Contrary to the global volcanic cooling trend in the first three years following these large tropical volcanic eruptions, an average 0.1 K global mean surface temperature rebound happened in the first post-eruption boreal winter (Xing et al., 2020). Such a global temperature rebound of the first Northern Hemisphere (NH) winter results from the atmospheric responses to the blockage of shortwave radiation, which induces an El Niño-like warming and a Eurasian warming caused by an enhanced polar vortex (Fig. 1b).

El Niño events were observed in the first boreal winters after these large tropical eruptions, except for the 1883

Krakatau eruption (Khodri et al., 2017). Due to the small sample size, the statistical significance cannot be established, and thus these El Niño events may also be attributable to internal variability (Self et al., 1997; Robock, 2000). However, long-term reconstruction analysis has suggested a hypothesis that large tropical eruptions can increase the probability of El Niño occurrence (Adams et al., 2003; McGregor and Timmermann, 2011; Liu et al., 2018a). Liu et al. (2018b) found that, over the last millennium, about 81% of tropical volcanic eruptions were followed by an El Niño-like sea surface temperature (SST) anomaly during the first post-eruption NH winter if the ocean before eruption had been in a neutral or La Niña condition. The 2019/20 winter did not witness a strong El Niño condition since not all the oceanic Niño indexes exceeded 0.5°C for five consecutive three-month periods. Therefore, there is an 83% (25/30) probability that an El Niño-like warming will occur in the 2020/21 winter if the Taal Volcano continues to eject large amounts of SO_2 into the stratosphere (Fig. 2a).

There are uncertainties in the prediction of the effects of volcanic eruptions on the El Niño occurrence with models. Numerical experiments of some individual models have reproduced the El Niño occurrence. The tropical eruption-induced El Niño in these models is related to several possible mechanisms: the ocean dynamic thermostat mechanism (Ohba et al., 2013; Predybaylo et al., 2017), the equatorward migration of the Intertropical Convergence Zone caused by reduced evaporation over cloudless subtropical regions (Lim et al., 2016), the land–ocean thermal contrast-induced westerly anomaly (Predybaylo et al., 2017), and the westerly response to suppressed West African monsoon and Warm Pool precipitation (Khodri et al., 2017; Chai et al., 2020). Another two factors may also affect the simulation of El Niño-like responses after tropical eruptions: the initial ocean condition and eruption strength. It is hard to replicate an El Niño when the initial ocean condition is already at an El Niño peak phase before the eruption (Liu et al., 2018b). Besides, the volcanic eruption has to be strong enough to excite an El Niño (Emile-Geay et al., 2008; Lim et al., 2016).

However, in contrast to the results obtained from experiments with the individual models, most models participating in phase 5 of the Coupled Model Intercomparison Project (CMIP5) (Xing et al., 2020), phase 3 of the Paleoclimate Modelling Intercomparison Project (Chai et al., 2020[a]), and CMIP6 (Fig. 2b) fail to produce an El Niño response in the first post-erup-

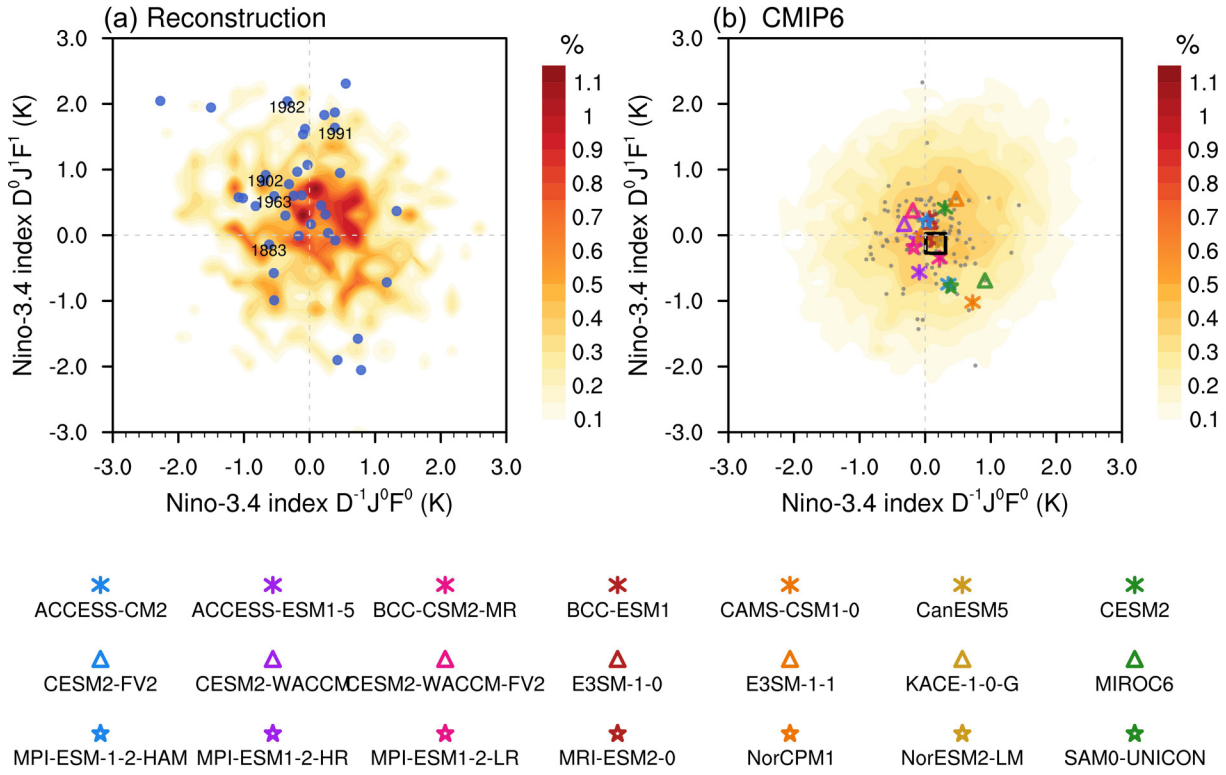

Fig. 2. Relationship between ENSO responses to tropical eruptions and initial ocean conditions. Scatterplots of Niño3.4 index anomalies (dots) during the winter before eruption versus the first winter after eruption in (a) reconstructed ENSO index for tropical eruptions over the past 1100 years, and in (b) CMIP6 for the five tropical eruptions since 1870. Shading indicates the density distribution of the internal mode of ENSO relative to the total sample number. As for the reconstructions, the recent large tropical eruptions since 1870 were selected based on Gao et al. (2008), and the remaining eruptions were based on Sigl et al. (2015). For the simulations, colored symbols denote the average of these five tropical eruptions for the ensemble mean of each model, and the black square is their multi-model mean.

[a] Chai, J., F. Liu, C. Xing, B. Wang, C. Gao, J. Liu, and D. Chen, 2020: A robust equatorial Pacific westerly response to tropical volcanism in multiple models: Wet region gets drier. *Climate Dyn.*, submitted.

tion winter. After tropical volcanic eruptions, the Niño3.4 SST warming cannot be reproduced against the uniform global volcanic cooling. In some models, however, a positive SST anomaly gradient in the equatorial Pacific with a positive sea surface height anomaly over the Niño3.4 region is simulated (Ding et al., 2014; Maher et al., 2015; Wang et al., 2018). This discrepancy demonstrates that there are limitations in the simulation of air–sea interaction in some models (Watanabe et al., 2011), and suggests the representation of local and remote signals in different El Niño–Southern Oscillation (ENSO) reconstructions (Li et al., 2011; Dee et al., 2020).

Volcanic eruptions can also affect the Eurasian winter temperature. A maximum 3°C surface temperature increase was observed over the Eurasian continent in the first winter following the 1991 Pinatubo eruption, which was associated with the global temperature rebound immediately after a volcanic eruption (Robock and Mao, 1992; Robock, 2002). Although this 1991/92 winter warming has been argued to have been caused by internal variability (Polvani et al., 2019), a Eurasian warming was also observed in the first NH winter after the other three tropical volcanic eruptions (Xing et al., 2020). This type of European warming was verified to have occurred after 15 major tropical eruptions in a 500-year multi-proxy reconstruction (Fischer et al., 2007).

The tropical volcanic eruption–Eurasian warming teleconnection is related to stratosphere–troposphere interaction. A tropical volcanic eruption can warm up the lower tropical stratosphere directly since the aerosol clouds absorb incoming near-infrared radiation and upwelling longwave radiation. Ozone in the polar region is depleted by volcanic aerosols by influencing stratospheric ozone photochemistry processes. Since stratospheric ozone absorbs solar radiation, ozone depletion will decrease temperatures in the polar region (Stenchikov et al., 2002). As shown in Fig. 3a, this low-latitude stratospheric warming and polar cooling increase the meridional temperature gradient over the NH, resulting in a strengthened polar vortex in the NH winter (Robock, 2000). This enhanced polar vortex, associated with a positive westerly anomaly, tends to warm up Eurasia by trapping tropospheric wave energy through reflection of planetary waves (Perlwitz and Graf, 1995; Butler et al., 2014). Most of the CMIP5 (Xing et al., 2020) and CMIP6 models (Fig. 3a) are able to simulate this low-latitude stratospheric warming induced by shortwave radiation absorption. The enhanced polar vortex in the models, however, is too weak compared to reanalysis (Fig. 3b), posing a challenge for the current simulation of stratospheric teleconnection.

Current GCMs are able to reproduce the direct responses to large tropical eruptions (Trenberth and Dai, 2007; Iles and Hegerl, 2014; Man and Zhou, 2014; Liu et al., 2016; Stevenson et al., 2016), but they still have difficulty simulating the delayed responses, which is determined by their performance in replicating internal variability (Ding et al., 2014; Maher et al., 2015; Wang et al., 2018; Liu et al., 2018a, 2018b; Xing et al., 2020).

The climate effects of the Taal Volcano eruption will depend on the magnitude of the eruption, especially on the amount of SO_2 ejected into the stratosphere to form volcanic aerosols. The Volcanic Explosivity Index (VEI)—a scale that represents the explosivity of an eruption event—consists of volcanically ejected materials, the height of the ash plume, and the type of eruption (Newhall and Self, 1982). Compared to the five large historical tropical eruptions, the Taal eruption is still too small, and its SO_2 amount is about two orders of magnitude smaller than those of the 1982 El Chichón and 1991 Pinatubo eruptions (Table 1), which means that the climate response to the current magnitude of the Taal eruption would be insignificant.

The Taal Volcano is still in an active phase, and the Philippine Institute of Volcanology and Seismology has sent out an alert over the Taal Volcano to warn that more explosive eruptions could happen. Since the 2019/20 winter was not in a strong El Niño condition, there is an 83% probability that an El Niño-like warming will occur in the 2020/21 winter if the magnitude of the continued Taal Volcano eruption or any other tropical volcanic eruption reaches a critical level where the VEI is greater than 3. Eurasian warming due to an enhanced polar vortex is also likely.

Data and methods

We used outputs during 1850 to 2015 from 131 historical runs of 21 coupled models (Table 2), which were the CMIP6 models released recently (https://esgf-node.llnl.gov). To avoid giving more weight to models with large ensembles, the multi-model ensemble mean was calculated for each model first. The observed surface air temperature was from the NASA Goddard Institute for Space Studies Surface Temperature Analysis (GISTEMP), version 3 (Lenssen et al., 2019), for the period 1870–2018. The geopotential height was derived from the Japanese 55-year Reanalysis (JRA-55) (Kobayashi et al., 2015). In this study, we used the reconstructed ENSO index from Li et al. (2011) over the period 900–1869, and the observed boreal-winter Niño3.4 index based on HadISST (Rayner et al., 2003) was adopted for the period 1870–2016. The volcanic eruptions over the past 1100 years were obtained from Sigl et al. (2015), which was based on the Greenland and Antarctic ice cores.

The effect of anthropogenic forcing was reduced through removing the linear trend of each variable. To separate volcanically forced climate responses from the climatological mean, the monthly mean of the five years preceding the eruptions

was removed. The Niño3.4 index used to represent El Niño events was calculated by the area mean over the Niño3.4 region (5°S–5°N, 170°–120°W). December–January–February was defined as boreal winter.

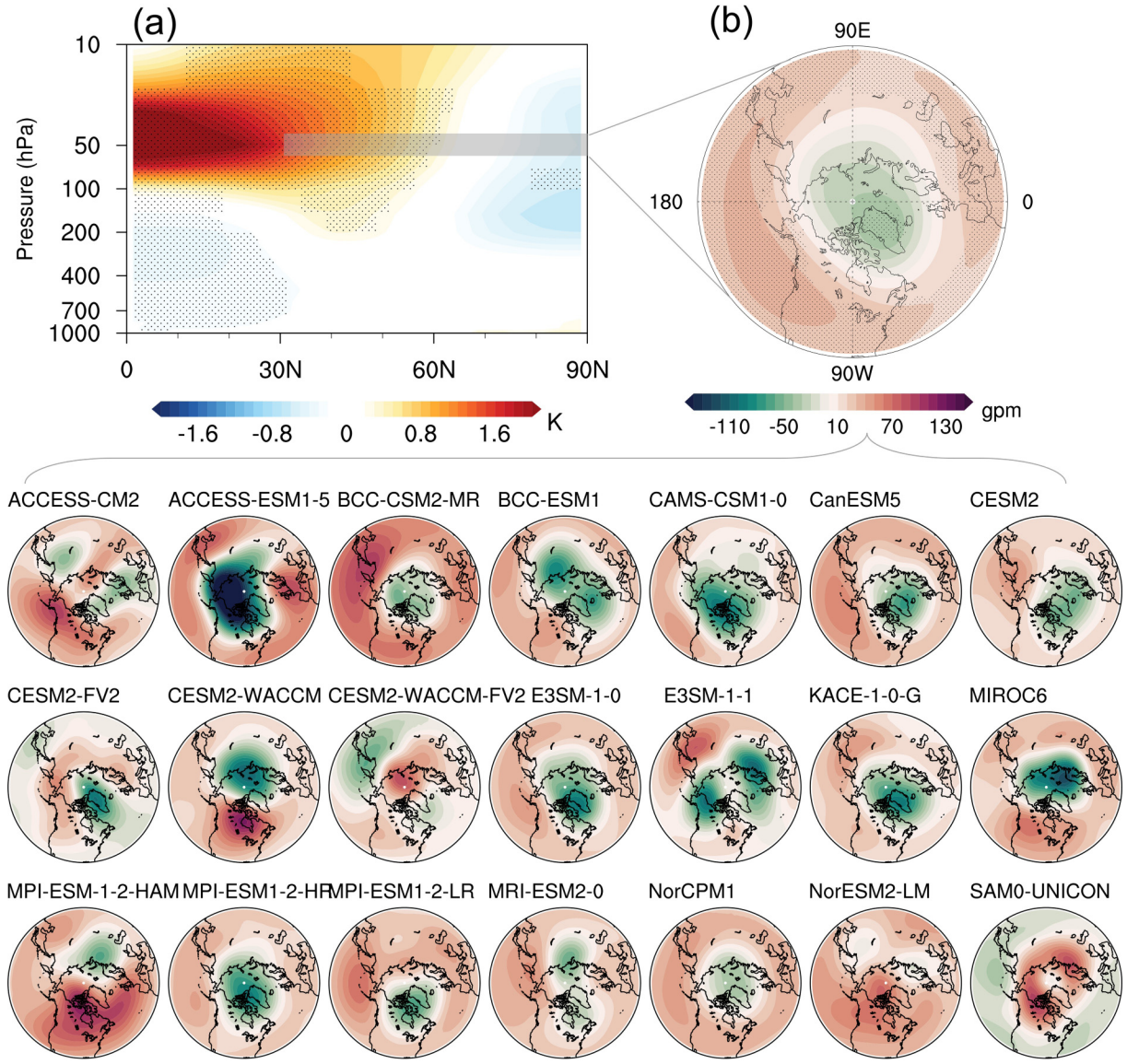

Fig. 3. Stratospheric responses to tropical volcanic eruptions in CMIP6. Composites of (a) zonally averaged temperature anomalies (shading) as a function of latitude and height, and (b) 50-hPa geopotential height anomalies (shading) in the first NH winter following the five tropical eruptions for the multi-model mean of the 21 CMIP6 models. The ensemble mean of each model is also shown in (b). Stippling denotes anomalies significant at the 95% confidence level.

Table 1. Information on the 2020 Taal eruption and the five strongest tropical eruptions over the past 150 years. The eruption date, location, aerosol loading, and Volcanic Explosivity Index (VEI) of each eruption are given. The SO_2 mass was obtained from Gao et al. (2008). For the 2020 Taal eruption, the accumulated SO_2 mass from 12–31 January was calculated by the Philippine Institute of Volcanology and Seismology (https://www.phivolcs.dost.gov.ph/index.php/taal-volcano-bulletin-menu/). The VEI of the Taal eruption is inferred from historical SO_2 loading and the eruption height.

Eruption	Date	Longitude/Latitude	SO_2 mass (Tg)	VEI
Krakatau	26–27 Aug 1883	6.1°S, 105.4°E	22	6
Santa Maria	24–25 Oct 1902	14.8°N, 91.6°W	4	5
Agung	17 Mar, 16 May 1963	8.3°S, 115.5°E	17	5
El Chichón	3–4 Apr 1982	17.4°N, 93.2°W	14	5
Pinatubo	15 Jun 1991	15.1°N, 120.4°W	30	6
Taal	12 Jan 2020	14.0°N, 120.6°E	0.019	3 (conjecture)

Table 2. Institution name, ID, and number of ensemble members of the CMIP6 models used in this study.

Institution	Institution ID	Model	Ensemble members
Commonwealth Scientific and Industrial Research Organisation, Aspendale, Australian Research Council Centre of Excellence for Climate System Science	CSIRO-ARCCSS	ACCESS-CM2	1
		ACCESS-ESM1-5	1
Beijing Climate Center	BCC	BCC-CSM2-MR	3
		BCC-ESM1	3
Chinese Academy of Meteorological Sciences	CAMS	CAMS-CSM1-0	2
Canadian Centre for Climate Modelling and Analysis	CCCma	CanESM5	25
National Center for Atmospheric Research	NCAR	CESM2	11
		CESM2-FV2	1
		CESM2-WACCM	3
		CESM2-WACCM-FV2	1
Lawrence Livermore National Laboratory, Livermore; Argonne National Laboratory, Argonne; Brookhaven National Laboratory; Los Alamos National Laboratory; Lawrence Berkeley National Laboratory; Oak Ridge National Laboratory; Pacific Northwest National Laboratory; Sandia National Laboratories	E3SM-Project	E3SM-1-0	5
		E3SM-1-1	1
National Institute of Meteorological Sciences/Korea Meteorological Administration	NIMS-KMA	KACE-1-0-G	3
Japan Agency for Marine-Earth Science and Technology, Atmosphere and Ocean Research Institute, National Institute for Environmental Studies, and RIKEN Center for Computational Science	MIROC	MIROC6	10
Max Planck Institute for Meteorology	MPI-M	MPI-ESM-1-2-HAM	2
		MPI-ESM1-2-HR	10
		MPI-ESM1-2-LR	10
Meteorological Research Institute	MRI	MRI-ESM2-0	5
Center for International Climate and Environmental Research, Norwegian Meteorological Institute, Nansen Environmental and Remote Sensing Center, Norwegian Institute for Air Research, University of Bergen, University of Oslo and Uni Research	NCC	NorCPM1	30
		NorESM2-LM	3
Seoul National University	SNU	SAM0-UNICON	1

Acknowledgements. This work was primarily supported by the National Natural Science Foundation of China (Grant Nos. 41975107 and 41971108). We would like to thank Mr. Faxin CHEN for providing the photo shown in Fig. 1a. We acknowledge the World Climate Research Programme's Working Group on Coupled Modelling, which is responsible for CMIP, and we thank the climate modeling groups for producing and making available their model outputs. This paper is ESMC Contribution No. 306.

REFERENCES

Adams, J. B., M. E. Mann, and C. M. Ammann, 2003: Proxy evidence for an El Niño-like response to volcanic forcing. *Nature*, **426**, 274–278, https://doi.org/10.1038/nature02101.

Bethke, I., S. Outten, O. H. Otterå, E. Hawkins, S. Wagner, M. Sigl, and P. Thorne, 2017: Potential volcanic impacts on future climate variability. *Nat. Clim. Change*, **7**, 799–805, https://doi.org/10.1038/nclimate3394.

Butler, A. H., L. M. Polvani, and C. Deser, 2014: Separating the stratospheric and tropospheric pathways of El Niño-Southern Oscillation teleconnections. *Environmental Research Letters*, **9**, 024014, https://doi.org/10.1088/1748-9326/9/2/024014.

Dee, S. G., K. M. Cobb, J. Emile-Geay, T. R. Ault, R. L. Edwards, H. Cheng, and C. D. Charles, 2020: No consistent ENSO response to volcanic forcing over the last millennium. *Science*, **367**, 1477–1481, https://doi.org/10.1126/science.aax2000.

Ding, Y. N., J. A. Carton, G. A. Chepurin, G. Stenchikov, A. Robock, L. T. Sentman, and J. P. Krasting, 2014: Ocean response to volcanic eruptions in Coupled Model Intercomparison Project 5 simulations. *J. Geophys. Res.*, **119**, 5622–5637, https://doi.org/10.1002/2013jc009780.

Emile-Geay, J., R. Seager, M. A. Cane, E. R. Cook, and G. H. Haug, 2008: Volcanoes and ENSO over the past millennium. *J. Climate*, **21**, 3134–3148, https://doi.org/10.1175/2007jcli1884.1.

Fischer, E. M., J. Luterbacher, E. Zorita, S. F. B. Tett, C. Casty, and H. Wanner, 2007: European climate response to tropical volcanic eruptions over the last half millennium. *Geophys. Res. Lett.*, **34**, L05707, https://doi.org/10.1029/2006gl027992.

Gagné, M. È., M. C. Kirchmeier-Young, N. P. Gillett, and J. C. Fyfe, 2017: Arctic sea ice response to the eruptions of Agung, El Chichón, and Pinatubo. *J. Geophys. Res.*, **122**, 8071–8078, https://doi.org/10.1002/2017jd027038.

Gao, C. C., A. Robock, and C. Ammann, 2008: Volcanic forcing of climate over the past 1500 years: An improved ice core-based index for climate models. *J. Geophys. Res.*, **113**, D23111, https://doi.org/10.1029/2008jd010239.

Iles, C. E., and G. C. Hegerl, 2014: The global precipitation response to volcanic eruptions in the CMIP5 models. *Environmental Research Letters*, **9**, 104012, https://doi.org/10.1088/1748-9326/9/10/104012.

Khodri, M., and Coauthors, 2017: Tropical explosive volcanic eruptions can trigger El Niño by cooling tropical Africa. *Nature Communications*, **8**, 778, https://doi.org/10.1038/s41467-017-00755-6.

Kobayashi, S., and Coauthors, 2015: The JRA-55 reanalysis: General specifications and basic characteristics. *J. Meteor. Soc. Japan*, **93**, 5–48, https://doi.org/10.2151/jmsj.2015-001.

Kravitz, B., and Coauthors, 2015: The Geoengineering Model Intercomparison Project Phase 6 (GeoMIP6): Simulation design and preliminary results. *Geoscientific Model Development*, **8**, 3379–3392, https://doi.org/10.5194/gmd-8-3379-2015.

Lenssen, N. J. L., G. A. Schmidt, J. E. Hansen, M. J. Menne, A. Persin, R. Ruedy, and D. Zyss, 2019: Improvements in the GISTEMP uncertainty model. *J. Geophys. Res.*, **124**, 6307–6326, https://doi.org/10.1029/2018jd029522.

Li, J. B., S.-P. Xie, E. R. Cook, G. Huang, R. D'Arrigo, F. Liu, J. Ma, and X.-T. Zheng, 2011: Interdecadal modulation of El Niño amplitude during the past millennium. *Nat. Clim. Change*, **1**, 114–118, https://doi.org/10.1038/nclimate1086.

Lim, H.-G., S.-W. Yeh, J.-S. Kug, Y.-G. Park, J.-H. Park, R. Park, and C.-K. Song, 2016: Threshold of the volcanic forcing that leads the El Niño-like warming in the last millennium: Results from the ERIK simulation. *Climate Dyn.*, **46**, 3725–3736, https://doi.org/10.1007/s00382-015-2799-3.

Liu, F., C. Xing, L. Y. Sun, B. Wang, D. L. Chen, and J. Liu, 2018b: How do tropical, northern hemispheric, and southern hemispheric volcanic eruptions affect ENSO under different initial ocean conditions? Geophys *Res. Lett.*, **45**, 13 041–13 049, https://doi.org/10.1029/2018gl080315.

Liu, F., J. Chai, B. Wang, J. Liu, X. Zhang, and Z. Y. Wang, 2016: Global monsoon precipitation responses to large volcanic eruptions. *Scientific Reports*, **6**, 24331, https://doi.org/10.1038/srep24331.

Liu, F., J. B. Li, B. Wang, J. Liu, T. Li, G. Huang, and Z. Y. Wang, 2018a: Divergent El Niño responses to volcanic eruptions at different latitudes over the past millennium. *Climate Dyn.*, **50**, 3799–3812, https://doi.org/10.1007/s00382-017-3846-z.

Liu, F., T. L. Zhao, B. Wang, J. Liu, and W. B. Luo, 2018c: Different global precipitation responses to solar, volcanic, and greenhouse gas forcings. *J. Geophys. Res.*, **123**, 4060–4072, https://doi.org/10.1029/2017jd027391.

Maher, N., S. McGregor, M. H. England, and A. Sen Gupta, 2015: Effects of volcanism on tropical variability. *Geophys. Res. Lett.*, **42**, 6024–6033, https://doi.org/10.1002/2015gl064751.

Man, W. M., and T. J. Zhou, 2014: Response of the East Asian summer monsoon to large volcanic eruptions during the last millennium. *Chinese Science Bulletin*, **59**, 4123–4129, https://doi.org/10.1007/s11434-014-0404-5.

McGregor, S., and A. Timmermann, 2011: The effect of explosive tropical volcanism on ENSO. *J. Climate*, **24**, 2178–2191, https://doi.org/10.1175/2010jcli3990.1.

Miller, G. H., and Coauthors, 2012: Abrupt onset of the Little Ice Age triggered by volcanism and sustained by sea-ice/ocean feedbacks. *Geophys. Res. Lett.*, **39**, L02708, https://doi.org/10.1029/2011gl050168.

Newhall, C. G., and S. Self, 1982: The volcanic explosivity index (VEI) an estimate of explosive magnitude for historical volcanism. *J. Geophys. Res.*, **87**, 1231–1238, https://doi.org/10.1029/JC087iC02p01231.

Niemeier, U., and S. Tilmes, 2017: Sulfur injections for a cooler planet. *Science*, **357**, 246–248, https://doi.org/10.1126/science.aan3317.

Ohba, M., H. Shiogama, T. Yokohata, and M. Watanabe, 2013: Impact of strong tropical volcanic eruptions on ENSO simulated in a coupled GCM. *J. Climate*, **26**, 5169–5182, https://doi.org/10.1175/jcli-d-12-00471.1.

Otterå, O. H., M. Bentsen, H. Drange, and L. L. Suo, 2010: External forcing as a metronome for Atlantic multidecadal variability. *Nature Geoscience*, **3**, 688–694, https://doi.org/10.1038/ngeo955.

Perlwitz, J., and H.-F. Graf, 1995: The statistical connection between tropospheric and stratospheric circulation of the northern hemisphere in winter. *J. Climate*, **8**, 2281–2295, https://doi.org/10.1175/1520-0442(1995)008<2281:tscbta>2.0.co;2.

Polvani, L. M., A. Banerjee, and A. Schmidt, 2019: Northern Hemisphere continental winter warming following the 1991 Mt. *Pinatubo eruption: Reconciling models and observations. Atmospheric Chemistry and Physics*, **19**, 6351–6366, https://doi.org/10.5194/acp-19-6351-2019.

Predybaylo, E., G. L. Stenchikov, A. T. Wittenberg, and F. R. Zeng, 2017: Impacts of a Pinatubo-size volcanic eruption on ENSO. *J. Geophys. Res.*, **122**, 925–947, https://doi.org/10.1002/2016jd025796.

Rayner, N. A., D. E. Parker, E. B. Horton, C. K. Folland, L. V. Alexander, D. P. Rowell, E. C. Kent, and A. Kaplan, 2003: Global analyses of sea surface temperature, sea ice, and night marine air temperature since the late nineteenth century. *J. Geophys. Res.*, **108**, 4407, https://doi.org/10.1029/2002JD002670.

Robock, A., 2000: Volcanic eruptions and climate. *Rev. Geophys.*, **38**, 191–219, https://doi.org/10.1029/1998RG000054.

Robock, A., 2002: Pinatubo eruption. *The climatic aftermath. Science*, **295**, 1242–1244, https://doi.org/10.1126/science.1069903.

Robock, A., and J. P. Mao, 1992: Winter warming from large volcanic eruptions. *Geophys. Res. Lett.*, **19**, 2405–2408, https://doi.org/10.1029/92gl02627.

Sato, M., J. E. Hansen, M. P. McCormick, and J. B. Pollack, 1993: Stratospheric aerosol optical depths, 1850-1990. *J. Geophys. Res.*, **98**, 22–22 994, https://doi.org/10.1029/93jd02553.

Schneider, D. P., C. M. Ammann, B. L. Otto-Bliesner, and D. S. Kaufman, 2009: Climate response to large, high-latitude and low-latitude volcanic eruptions in the Community Climate System Model. *J. Geophys. Res.*, **114**, D15101, https://doi.org/10.1029/2008jd011222.

Sear, C. B., P. M. Kelly, P. D. Jones, and C. M. Goodess, 1987: Global surface-temperature responses to major volcanic eruptions.

Nature, **330**, 365–367, https://doi.org/10.1038/330365a0.

Self, S., M. R. Rampino, J. Zhao, and M. G. Katz, 1997: Volcanic aerosol perturbations and strong El Niño events: No general correlation. *Geophys. Res. Lett.*, **24**, 1247–1250, https://doi.org/10.1029/97gl01127.

Sigl, M., and Coauthors, 2015: Timing and climate forcing of volcanic eruptions for the past 2:500 years. *Nature*, **523**, 543–549, https://doi.org/10.1038/nature14565.

Slawinska, J., and A. Robock, 2018: Impact of volcanic eruptions on decadal to centennial fluctuations of arctic sea ice extent during the last millennium and on initiation of the little ice age. *J. Climate*, **31**, 2145–2167, https://doi.org/10.1175/jcli-d-16-0498.1.

Stenchikov, G., A. Robock, V. Ramaswamy, M. D. Schwarzkopf, K. Hamilton, and S. Ramachandran, 2002: Arctic Oscillation response to the 1991 Mount Pinatubo eruption: Effects of volcanic aerosols and ozone depletion. *J. Geophys. Res.*, **107**, 4803, https://doi.org/10.1029/2002jd002090.

Stevenson, S., B. Otto-Bliesner, J. Fasullo, and E. Brady, 2016: "El Niño Like" hydroclimate responses to last millennium volcanic eruptions. *J. Climate*, **29**, 2907–2921, https://doi.org/10.1175/jcli-d-15-0239.1.

Tilmes, S., and Coauthors, 2013: The hydrological impact of geoengineering in the Geoengineering Model Intercomparison Project (GeoMIP). *J. Geophys. Res.*, **118**, 11 036–11 058, https://doi.org/10.1002/jgrd.50868.

Tilmes, S., and Coauthors, 2019: Reaching 1.5°C and 2.0°C global surface temperature targets using stratospheric aerosol geoengineering. *Earth System Dynamics*, https://doi.org/10.5194/esd-2019-76.

Trenberth, K. E., and A. G. Dai, 2007: Effects of Mount Pinatubo volcanic eruption on the hydrological cycle as an analog of geoengineering. *Geophys. Res. Lett.*, **34**, L15702, https://doi.org/10.1029/2007gl030524.

Wang, T., D. Guo, Y. Q. Gao, H. Wang, F. Zheng, Y. Zhu, J. Miao, and Y. Hu, 2018: Modulation of ENSO evolution by strong tropical volcanic eruptions. *Climate Dyn.*, **51**, 2433–2453, https://doi.org/10.1007/s00382-017-4021-2.

Watanabe, M., M. Chikira, Y. Imada, and M. Kimoto, 2011: Convective control of ENSO simulated in MIROC. *J. Climate*, **24**, 543–562, https://doi.org/10.1175/2010jcli3878.1.

Xing, C., F. Liu, B. Wang, D. L. Chen, J. Liu, and B. Liu, 2020: Boreal winter surface air temperature responses to large tropical volcanic eruptions in CMIP5 models. *J. Climate*, **33**, 2407–2426, https://doi.org/10.1175/jcli-d-19-0186.1.

Xu, Y. Y., and Coauthors, 2020: Climate engineering to mitigate the projected 21st-century terrestrial drying of the Americas: Carbon Capture vs. Sulfur Injection? Earth System Dynamics, https://doi.org/10.5194/esd-2020-2.

Zanchettin, D., C. Timmreck, H.-F. Graf, A. Rubino, S. Lorenz, K. Lohmann, K. Krüger, and J. H. Jungclaus, 2011: Bi-decadal variability excited in the coupled ocean-atmosphere system by strong tropical volcanic eruptions. *Climate Dyn.*, **39**, 419–444, https://doi.org/10.1007/s00382-011-1167-1.

Zanchettin, D., O. Bothe, H. F. Graf, S. J. Lorenz, J. Luterbacher, C. Timmreck, and J. H. Jungclaus, 2013: Background conditions influence the decadal climate response to strong volcanic eruptions. *J. Geophys. Res.*, **118**, 4090–4106, https://doi.org/10.1002/jgrd.50229.

Zuo, M., T. J. Zhou, and W. M. Man, 2019: Wetter global arid regions driven by volcanic eruptions. *J. Geophys. Res.*, **124**, 13 648–13 662, https://doi.org/10.1029/2019jd031171.